CrossMark

TECHNICAL PAPER

Size control of $CH_3NH_3PbBr_3$ perovskite cuboid fine crystals synthesized by ligand-free reprecipitation method

Kazuki Umemoto[1] · Yong-Jin Pu[1] · Cigdem Yumusak[2] · Markus Clark Scharber[2] · Matthew Schuette White[3] · Niyazi Serdar Sariciftci[2] · Tsukasa Yoshida[1] · Jun Matsui[1] · Hiroshi Uji-i[4] · Akito Masuhara[1]

Abstract Cuboid fine crystals of methylammonium lead tribromide ($MAPbBr_3$) perovskite have been synthesized by ligand-free reprecipitation method employing N,N-dimethylformamide (DMF) and 1,2,4-trichlorobenzene (TCB) as good and poor solvents, respectively. A small amount of DMF solution dissolving precursor chemicals of $MAPbBr_3$ was rapidly injected to TCB under vigorous stirring to promote the reprecipitation. Mean crystal size could be varied between 70 and 600 nm by controlled addition of cyclohexane to TCB, since cyclohexane has been found to play a role to retard droplet diffusion. Cyclohexane was miscible with TCB but poorly miscible with DMF. Thus, addition of cyclohexane to TCB retarded diffusion of the injected droplets of DMF solution for reprecipitation of $MAPbBr_3$. As the mixing of good and poor solvents was retarded, the recrystallization process was also slowed down, resulted in a small number of nuclei and their growth to large size. Moreover, extreme addition of cyclohexane has resulted in a hollow core spherical particles of $MAPbBr_3$ due to aggregation of the cuboid fine crystals at the boundary between the added droplet and the poor solvent, so that the spheres formed preserving the shape of the droplet. Due to the limited miscibility of cyclohexane to DMF, increasing the cyclohexane content resulted in reduced rate of diffusion of the injected $MAPbBr_3$ solution, thus increasing the size of the crystals.

1 Introduction

Organic/inorganic hybrid lead halide perovskite $CH_3NH_3PbX_3$ (X = Cl, Br, and I) crystals are emerging as the solution processable light absorber materials in highly efficient solar cells (Green et al. 2016). These perovskite crystals exhibit attractive features such as wide-range color tunability adjusted by halide ions in perovskite crystal structure (Zhang et al. 2015), high absorption coefficient in visible range (Miyasaka 2015), long carrier diffusion length of free carriers (Dong et al. 2015), and the small

✉ Akito Masuhara
masuhara@yz.yamagata-u.ac.jp

Kazuki Umemoto
tnk94675@st.yamagata-u.ac.jp

Yong-Jin Pu
pu@yz.yamagata-u.ac.jp

Cigdem Yumusak
cigdem.yumusak@jku.at

Markus Clark Scharber
markus_clark.scharber@jku.at

Matthew Schuette White
mwhite25@uvm.edu

Niyazi Serdar Sariciftci
serdar.sariciftci@jku.at

Tsukasa Yoshida
yoshidat@yz.yamagata-u.ac.jp

Jun Matsui
jun_m@sci.kj.yamagata-u.ac.jp

Hiroshi Uji-i
hiroshi.ujii@chem.kuleuven.ac.be

[1] Yamagata University, Johan 4-3-16, Yonezawa, Yamagata 992-8510, Japan

[2] Kepler University Linz, Altenberger Street 69, 4040 Linz, Austria

[3] University of Vermont, Burlington, VT 054050125, USA

[4] University of Leuven, Celestijnenlaan 200f - box 2404, 3001 Leuven, Belgium

exciton binding energy (Lin et al. 2015). They are therefore promising for their applications in the state-of-the-art technologies such as light emitting diodes (Tan et al. 2014), lasers (Zhang et al. 2014), field effect transistors (Chin et al. 2015), and efficient optical devices (Sutherland and Sargent 2016), in addition to solar cells.

Recently, quantum size effects in nanocrystals (NCs) of MAPbBr$_3$ has also been investigated, owing to the establishment of various preparation methods of NCs. Kojima et al. have succeeded in suppressing rapid crystal growth of MAPbBr$_3$ by employing a mesoporous scaffold of Al$_2$O$_3$ (Kojima et al. 2012). Schmidt et al. have prepared colloidal MAPbBr$_3$ NCs based on a non-template strategy, in which they used several additives such as long chain ammonium bromide, oleic acid, and octadecene to control the crystal growth (Schmidt et al. 2014). These reports revealed superb luminescent properties of MAPbBr$_3$ NCs.

We have previously developed reprecipitation method to prepare various kinds of organic NCs (Tan et al. 2008) and discussed the mechanism of nano-crystallization (Shito and Masuhara 2015). In this process, shapes, sizes and structures of NCs can be flexibly controlled simply by changing the preparation conditions without relying on use of surfactants (Masuhara et al. 2009). Recently, Tachikawa et al. reported ligand-free reprecipitation of MAPbBr$_3$ NCs and observed their photoluminescence characteristics as investigated by single-particle spectroscopy (Tachikawa et al. 2015). Nanocrystals size is a key factor in determining the photoluminescence peak. The ligand-free synthetic approach has also turned out to be useful to study the influence of surface passivation by Lewis bases, as the surface of the synthesized MAPbBr$_3$ NCs was not covered with ligands.

In this work, we have focused on ligand-free reprecipitation of MAPbBr$_3$ crystals to establish methods to control their sizes and shape. In this study, cuboid MAPbBr$_3$ fine crystals were successfully synthesized by employing N,N-dimethylformamide (DMF) and 1,2,4-trichlorobenzene (TCB) as good and poor solvents, respectively. Addition of cyclohexane to TCB has turned out to be an effective means to control the crystal size and overall morphology of the nanoparticles. The range of the size and shape control, crystallographic characteristics of the products have been identified, leading us to a proposal of the mechanism of nanocrystallization in this system.

2 Experimental

2.1 Materials

PbBr$_2$ powder (99.999%) was purchased from Aldrich. Methylammonium bromide (MABr) powder (98.0%), DMF, TCB, and cyclohexane were purchased from Wako

Pure Chemical Industries. All the chemicals were used without purification.

2.2 Preparation of MAPbBr$_3$ fine crystals

Stoichiometric amounts of precursor chemicals, namely, 5.6 mg PbBr$_2$ and 18.4 mg MABr were dissolved into 0.5 ml of DMF to form a solution of MAPbBr$_3$. In standard experiments, a given amount (60 μl) of the MAPbBr$_3$ solution was injected into a 3 ml of TCB at room temperature under vigorous stirring, causing a rapid change of the color of the solution from colorless to yellow, indicating formation of fine crystals. The dispersion was filtered with a membrane filter and the filtered solid sample was dried under air at room temperature. Size and shape control of the fine crystals have been achieved by mixing cyclohexane into TCB up to a ratio of TCB: cyclohexane = 0.3: 2.7 in ml.

2.3 Characterization

The products were observed by a JEOL JSM-6700F scanning electron microscope (SEM). X-ray diffraction (XRD) patterns of the samples were measured on a Rigaku Smart-Lab (using Cu Kα radiation at 45 kV and 200 mA).

3 Results and discussion

Fine crystals synthesized by the reprecipitation method described above were of cuboid shape with sharp crystal facets. Figure 1 shows SEM images of the products, representing the smallest [70 nm, (a) and (b)] and the largest [600 nm, (c) and (d)] MAPbBr$_3$ fine crystals. Despite of their significant difference of the size, they both are MAPbBr$_3$ perovskite of the same quality without inclusion of DMF molecules used as the good solvent, as evidenced in their XRD patterns conforming to the perovskite single phase (Fig. 2). Size control was achieved without changing these features simply by adding cyclohexane to TCB. For the largest 600 nm cube, a mixture of 0.5 ml TCB and 2.5 ml cyclohexane was employed as the poor solvent.

The variation of the crystal size is plotted as a function of volume ratio of cyclohexane in the poor solvent in Fig. 3. When the vol % of cyclohexane is below 20%, the small crystal sizes of ca. 70 nm was maintained. Upon further increase of cyclohexane, the crystal size gradually increased. It rather abruptly jumped up to approach 600 nm between 50 and 65% of cyclohexane.

Our previous studies on reprecipitation have revealed that the control of miscibility between good and poor solvents is the key factor to control the size and morphology of the NCs (Tan et al. 2008). Cyclohexane is miscible with TCB but poorly miscible with DMF. Thus, addition
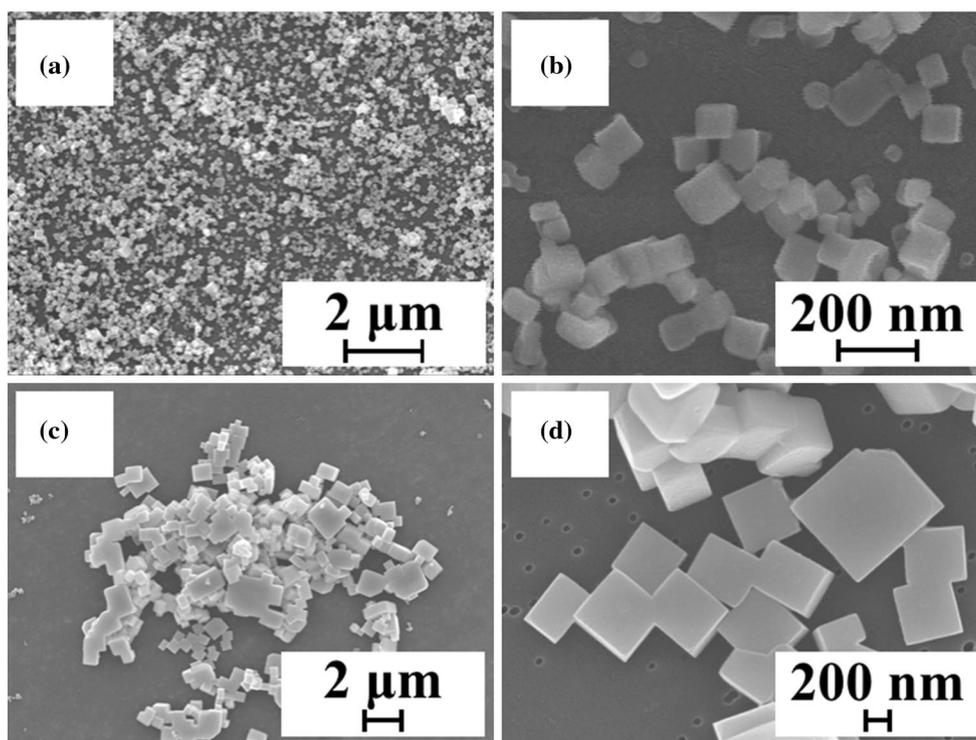
Fig. 1 SEM image of MAPbBr$_3$ fine crystals. **a**, **b** Using the TCB and **c**, **d** using the TCB-Cyclohexane mixed solvent as a poor medium
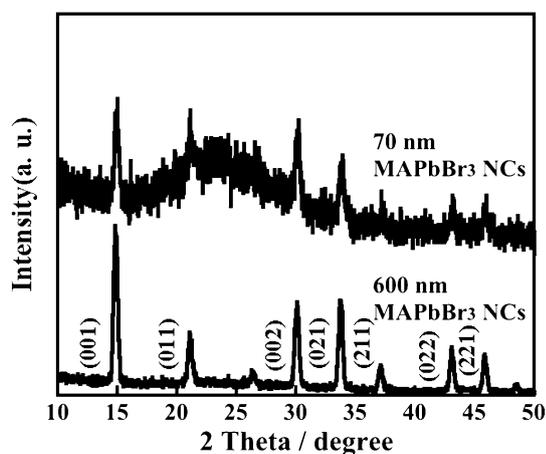

Fig. 2 XRD patterns of 70 nm and 600 nm MAPbBr$_3$ crystals, respectively
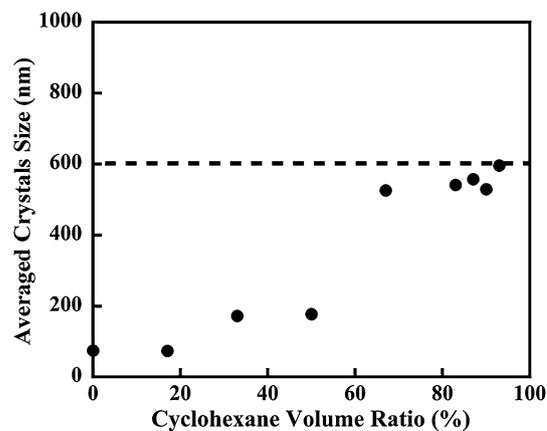

Fig. 3 Relationship between obtained MAPbBr$_3$ crystals sizes and cyclohexane volume ratio. *Dashed line* represents the maximum attained crystal size

of cyclohexane to TCB retards diffusion of the injected droplets of DMF solution for reprecipitation of MAPbBr$_3$. As the mixing of good and poor solvents is retarded, the recrystallization process is also slowed down, resulting in a small number of nuclei and their growth to large size. Another important factor is the viscosity of the good solvent. In our previous research, hollow-core spherical particles formed as an assembly of C$_{60}$ NCs was achieved by employing *trans*-decahydronaphthalene with a high

viscosity (2.27 mPa s) as a good solvent. Since the droplet injected to the poor solvent diffuse slowly, nanocrystallization takes place only at the boundary between the added droplet and the poor solvent, so that such a hollow sphere preserving the shape of the added droplet could be formed. Extreme addition of cyclohexane to TCB indeed resulted in the formation of such hollow-core spheres. Figure 4 shows SEM images of assemblies of MAPbBr$_3$ fine crystals in a hollow-core spherical shape obtained in a poor solvent
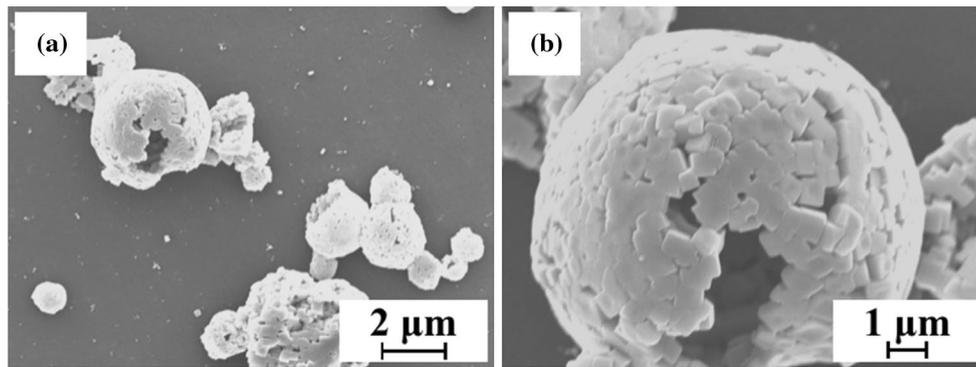
Fig. 4 a SEM images of MAPbBr$_3$ crystals with hollow spherical structures. **b** Enlarged view

containing only 0.3 ml of TCB and 2.7 ml of cyclohexane. Cuboid NCs of MAPbBr$_3$ with about 530 nm size aggregate to form the shell of the spheres.

Based on these observations for the transition of the crystal size as well as the formation of the hollow sphere,

and the results of our previous investigations (Shito and Masuhara 2015), we propose the following mechanism of MAPbBr$_3$ nanocrystallization in the present system, schematically illustrated in Fig. 5. When a compatible set of good and poor solvents is employed, namely, DMF and
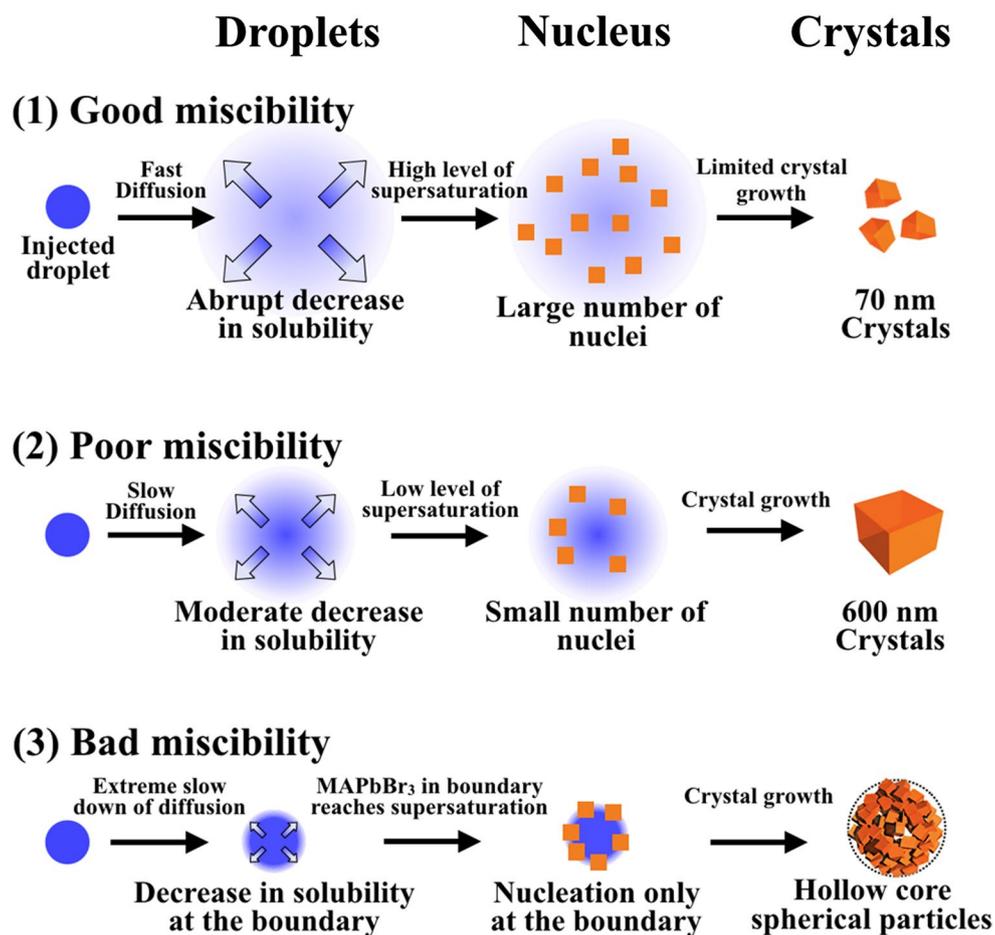

Fig. 5 Schematic illustrations of proposed mechanisms for MAPbBr$_3$ fine crystals. *1* 70 nm MAPbBr$_3$ NCs, *2* 600 nm MAPbBr$_3$ Crystals and *3* MAPbBr$_3$ crystals with hollow spherical structures

TCB which are nicely miscible, the injected DMF solution dissolving MAPbBr$_3$ smoothly diffuse into TCB. Such a situation corresponds to Fig. 5(1) in which abrupt decrease of the solubility of MAPbBr$_3$ results in a formation of a large number of nuclei. However, they cannot grow large because source chemicals are quickly depleted. Thus, a large number of tiny NCs are formed. When the compatibility of the solvents is worsened, namely, when cyclohexane with limited miscibility to DMF is added to the poor solvent, the diffusion of the MAPbBr$_3$ solution should be retarded [illustrated as Fig. 5(2)]. As the solubility is only gradually reduced, in other words, only a moderate level of supersaturation of MAPbBr$_3$ is reached, a small number of nuclei can only be formed. These nuclei, however, have chances to grow larger due to continuous supply of the source ions from the injected droplet acting as the chemical reservoir. Thus, relatively large sized cuboid crystals could be formed. Upon extreme addition of cyclohexane [the situation illustrated as Fig. 5(3)], the injected solution is expected to survive as droplets in the mixture for some time, due to the significantly reduced miscibility of the good and poor solvents. Then, the recrystallization of MAPbBr$_3$ is to take place at the boundary between such droplets and the poor solvents. Each one of the cuboids can grow fairly large due to supply of the source chemicals from the droplets. But more importantly, crystallization in such a confined space results in their interconnection to form a shell that copies the shape of the droplets. This way, the observed assemblies of the cuboid fine crystals into hollow-core spheres are formed.

4 Conclusion

Cuboid fine crystals of MAPBBr$_3$ have been successfully synthesized by a ligand-free reprecipitation method. Mean crystal sizes were controlled between 70 and 600 nm by addition of cyclohexane to TCB used as the poor solvent. Due to the limited miscibility of cyclohexane to DMF, increasing the cyclohexane content resulted in reduced rate of diffusion of the injected MAPbBr$_3$ solution, thus increasing the size of the crystals. With an extreme addition of cyclohexane, hollow-core spheres made as assemblies of the cuboid MAPbBr$_3$ fine crystals were formed. A mechanism for such a transition of the size and shape has been proposed. Size controlled synthesis MAPbBr$_3$ crystals in distinctive cuboid shape by the present reprecipitation method can provide new synthetic route to photoactive materials in solar cells as well as in various other optoelectronic devices.

References

Chin XY, Cortecchia D, Yin J, Annalisa B, Soci C (2015) Lead iodide perovskite light-emitting field-effect transistor. Nat Commun 6:1–9

Dong Q, Fang Y, Shao Y, Mulligan P, Qiu J, Cao L, Huang J (2015) Solar cells. Electron-hole diffusion lengths >175 μm in solution-grown CH$_3$NH$_3$PbI$_3$ single crystals. Science 347:967–970

Green MA, Emery K, Hishikawa Y, Warta W, Dunlop ED, Levi DH, Ho-Baillie AWY (2016) Solar cell efficiency tables (version 49). Prog Photovot Res Appl 25:3–13

Kojima A, Ikegami M, Teshima K, Miyasaka T (2012) Highly luminescent lead bromide perovskite nanoparticles synthesized with porous alumina media. Chem Lett 41:397–399

Lin Q, Armin A, Nagiri RCR, Burn PL, Meredith P (2015) Electro-optics of perovskite solar cells. Nat Photon 9:106–112

Masuhara A, Tan Z, Kasai H, Nakanishi H, Oikawa H (2009) Fullerene fine crystals with unique shapes and controlled size. Jpn J Appl Phys 48:0502061–0502063

Miyasaka T (2015) Perovskite photovoltaics: rare functions of organo lead halide in solar cells and optoelectronic devices. Chem Lett 44:720–729

Schmidt LC, Pertegas A, Gonzalez-Carrero S, Malinkiewicz Q, Agouram S, Malinkiewicz O, Espallargas GM, Bolink HJ, Galian RE, Perez-Prieto J (2014) Nontemplate synthesis of CH$_3$NH$_3$PbBr$_3$ perovskite nanoparticles. J Am Chem Soc 136:850–853

Shito K, Ito N, Masuhara A (2015) Investigation of C$_{60}$ nanocrystallization processes in reprecipitation method using low compatibility solvents. Jpn J Appl Phys 54:06FK01–06FK05

Sutherland BR, Sargent EH (2016) Perovskite photonic sources. Nat Photon 10:295–302

Tachikawa T, Karimata I, Kobori Y (2015) Surface charge trapping in organolead halide perovskites explored by single-particle photoluminescence imaging. J Phys Chem Lett 6:3195–3201

Tan Z, Masuhara A, Kasai H, Nakanishi H, Oikawa H (2008) Multi-branched C$_{60}$ micro/nanocrystals fabricated by reprecipitation method. Jpn J Appl Phys 47:1426–1428

Tan ZK, Moghaddam RS, Lai ML, Docampo P, Higler R, Deschler F, Price M Sadhanala, Pazous ALM, Credgington D, Hanusch F, Bein T, Snaith HJ, Friend RH (2014) Bright light-emitting diodes based on organometal halide perovskite. Nat Nanotechnol 9:687–892

Zhang Q, Ha ST, Liu X, Sum TC, Xiong Q (2014) Room-temperature near-infrared high-Q perovskite whispering-gallery planar nanolasers. Nano Lett 14:5995–6001

Zhang F, Zhong HZ, Chen C, Wu XG, Hu XM, Huang HL, Han JB, Zou BS, Dong YP (2015) Brightly luminescent and color-tunable colloidal CH$_3$NH$_3$PbX$_3$ (X = Br, I, Cl) quantum dots: potential alternatives for display technology. ACS Nano 9:4533–4542